www.czasopisma.pan.pl PAN POLSKA AKADEMIA NAUK www.journals.pan.pl

Arch. Metall. Mater. **64** (2019), 1, 431-436

DOI: 10.24425/amm.2019.126269

Z. ZIMNIAK*#, D. DOBRAS*

ELECTROPLASTIC EFFECT OF HIGH MANGANESE AUSTENITIC STEEL

The article presents the results of the investigations performed on high manganese austenitic steel which underwent the test of uniaxial tension, with the application of electric current impulses. The application of low voltage impulse alternating current of high intensity during the plastic deformation of the examined steel caused the occurrence of the electroplastic effect, which changed the shape of the stress-strain curve. A drop of flow stress and elongation of the tested material was observed in the case of the application of electric current impulses, in respect of the material stretched without such impulses and stretched at an elevated temperature. The analysis of the morphology of the fractures showed differences between the samples tested under the particular conditions. An analysis of the alloy's microstructure was also performed under different conditions. The application of electric current impulses can have a significant influence on the reduction of the forces in the plastic forming processes for this type of steel.

Keywords: electroplastic effect, high manganese steel, TWIP effect

1. Introduction

It is commonly known that the application of electric current impulses with a properly high intensity and the appropriate duration time can increase the plasticity and reduce the flow stress of the plastically deformed material. This phenomenon is called the electroplastic effect (EPE) [1-2]. It is assumed that the electric current flowing through the material affects on the existing dislocations and their interactions with the obstacles present in their way. Such effect makes it easier for the dislocations to cross over the obstacles, thus increasing the material's plasticity. In his works, Conrad [1-2] points to the significance of the dislocation-electron interaction, which can also be responsible for the observed phenomena. In turn, Molotskii [3] states that the electric current flowing through the alloy induces magnetic field, which makes it easier for the dislocations to detach from the paramagnetic obstacles and pass through them.

Although the theoretical basis of this phenomenon is still little known, the application of electric current impulses in the plastic forming processes brings very interesting results. For example, Song et al. [4] succeeded in increasing the engineering strain of aluminum alloy 5052-H32 from 11,4 wt.% to 34,8 wt.% in respect of the material stretched without the application of electric current impulses, and in the case of magnesium alloy AZ31B-O – from 25 wt.% up to as much as 41 wt.%. In both cases, there was a drop of the yield stress. Lesiuk at al. [5] investigated the effect of the application of electric current impulses on the fatigue strength of steel AISI 304, which was successfully increased by the average of 11 wt.%. Zimniak et al. [6] studied the occurrence of EPE in the process of drawing wires made of pure copper, obtaining a lower drawing load and better plastic properties of the obtained products.

Owing to their interesting properties, high strength and good plasticity, austenitic steels have been a common subject of research related to the electroplastic effect. Also as a result of the studies of the electroplastic effect, in the process of drawing wires made of chromium-nickel stainless steel, a significant reduction of the drawing load was obtained, as well as an improvement of the quality of the obtained products and an increase of their plasticity, with a simultaneous drop of their tensile strength [7-8]. Breda et al. [9] performed tensile tests on steel AISI 316L; however, they applied direct current, obtaining lower flow stress and, at the same time, a smaller elongation.

This article presents the investigations performed on high manganese austenitic steel, type X50MnAl15-2, with the effect of reinforcement through mechanical twinning (TWIP – twinning-induced plasticity). High manganese TWIP steels belong to the group of Advanced High Strength Steel (AHSS) and they are hoped to be used e.g. as: motorcar body components, as, owing to the TWIP effect, they characterize in an increased storage of cold plastic deformation energy. They also characterize in a good combination of high mechanical properties and good plasticity. However, their price is relatively high compared to the conventional steels from the AHSS group. An additional problem connected with the forming of elements made of this alloy is the necessity of using high force in the plastic treatment processes [10-12]. And so, the aim of this study is to examine the behaviour of TWIP steels during plastic deformation with the application

* WROCŁAW UNIVERSITY OF SCIENCE AND TECHNOLOGY, DEPARTMENT OF METAL FORMING AND METROLOGY, 5 ŁUKASIEWICZA STR., 50-370 WROCŁAW, POLAND

Corresponding author: zbigniew.zimniak@pwr.edu.pl

of electric current impulses. Such a solution can undoubtedly contribute to a reduction of the flow stress of the examined material, and, as a result, of the force needed for the plastic deformation, and also to a reduction of the energy consumption.

2. Experimental

2.1. Materials

High manganese austenitic steel sheet X50MnAl15-2, thickness 1,5 mm, was selected for the presented studies. The chemical composition of the alloy, measured by means of a chemical composition analyzer emission spectrometer LECO GDS500A, has been given in Table 1. A properly high content of carbon, manganese and aluminum made it possible to obtain steel with the stacking fault energy (SFE) ensuring the occurrence of plastic strain induced twinning (TWIP). The SFE of the examined steel also makes possible the occurrence of a martensitic transformation induced by plasticity; however, not with the applied deformation rate [11]. The samples were prepared through laser cutting and made in line with the metal sheet rolling direction. The gage width of the sample equalled 12 mm and its gage length was 75 mm.

TABLE 1

Chemical composition of steel X50MnAl15-2

Element	C	Mn	Si	P	S	Cr	Al	Fe
wt.%	0,532	14,5	0,142	0,0018	0,0007	0,5659	2,11	Residue

2.2. Methods

The tensile tests of the examined material were performed on an INSTRON 3369 tensile machine, with the deformation rate equalling $2*10^{-2}$ s^{-1}. The electric current impulses were provided by means of a constructed high current impulse generator. For the construction of the generator, 4 super-capacitors were used, with the total capacity of 14000 F, and its maximal working voltage equalled 2,7 V. An oscilloscope and a function generator were applied to control the current impulses. The shape of the generated impulses has been shown in Figure 1, where t_d is the duration time of an impulse and t_p is the time period.

The intensity of the current flowing through the samples was measured by means of the Rogowski Coil Power Electronic Measurements UK. The maximal temperature reached by the samples during the tensile test was recorded by a thermovision camera FLIR T440. The electric current impulses were applied throughout the whole duration time of the sample's stretching. The examined material was separated with insulators from the remaining part of the tensile machine. The applied current parameters have been included in Table 2. The discharge voltage for each test was the same and equalled 2,53 V. In order to separate the effect of the temperature coming only from the flowing current, the tensile tests were performed also in a thermal chamber, without current flow, with the use of a ZWCIK 1478 tensile machine. An analysis of the morphology of the fractures was conducted by means of a scanning electron microscope (SEM) VEGA3 TESCAN. The material test samples were etched in nital or aqua regia. The material tests were performed with the use of a light microscope Olympus GX51 and NIKON ECLIPSE MA200.

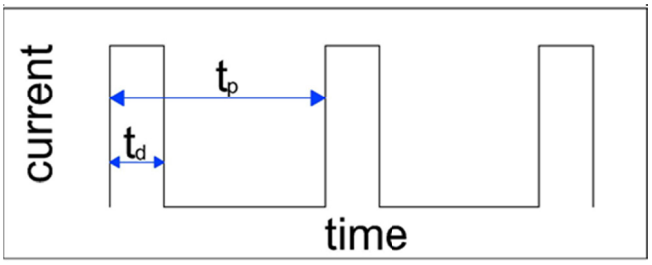

Fig. 1. Schematic diagram of the current impulse application

TABLE 2

Experimental parameters

No.	t_d	t_p
1	80 µs	400 µs
2	100 µs	1 ms
3	500 µs	2 ms
4	1 ms	10 ms
5	10 ms	100 ms
6	50 ms	500 ms
7	50 ms	300 ms
8	50 ms	150 ms

3. Results and discussion

In the as-received state, material is characterized by a fine-grained structure, with clearly visible banding (Fig. 2). Banding is an effect of the rolling process. The observed grain size is

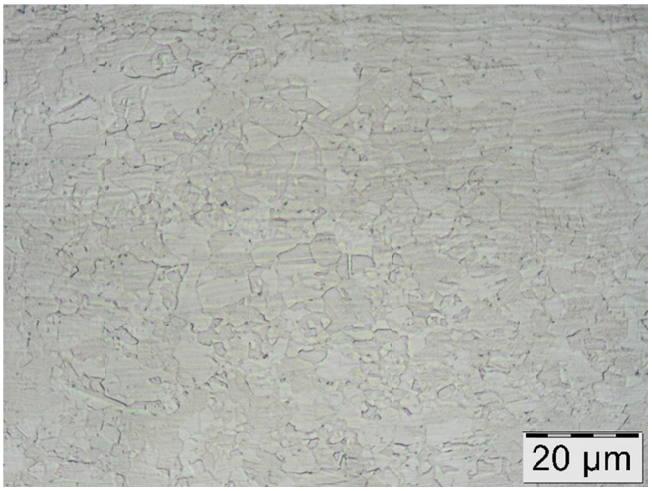

Fig. 2. Microstructure of the as-received material of steel X50MnAl15-2, LOM, etched in aqua regia

within the range of a few to over a dozen micrometers and the twin boundaries are present within the particular austenite grains. The presence of ferrite and strain-induced martensite was not observed [9,12].

The application of electric current impulses was in line with the diagram presented in Fig. 1 and the test parameters have been given in Table 2. The density ρ of the current which was flowing through the examined material in the particular tests has been shown in Table 3. The flowing current was measured by means of the Rogowski coil, and the obtained value was divided by the surface area of the cross-section of the sample, in order to obtain the current density. The maximum temperature values *T* recorded during the stretching of the particular samples until the moment of fracture have been included in Table 3.

A comparison of the material's stress-stain curves, both in the case of the application of electric current impulses and without it, at ambient temperature, has been shown in Figs. 3-5. Due to a large number of lines and for better readability, the obtained data have been divided into three groups.

As it has been demonstrated in Figure 3, the application of very short impulses caused a slight drop of stress and a reduction of elongation. With the increase of the impulse length, the drop of stress and the elongation reduction were increasing (Fig. 4). At the same time, an increase of the current density as well as increase of the tested material's temperature was observed – Table 3.

As it has been shown in Figure 5, the presence of characteristic "serrations" on the stress-strain curve was observed when the impulse's duration time and the period were increased. Such a behaviour should be explained by the fact that, at the moment of applying the electric current impulse, a drop of flow stress takes place (stress-drop), whereas, during the pause between the impulses, the material begins to strain-hardening behaviour again, which is a commonly known phenomenon [13]. A significant drop of stress and elongation were observed when the frequency of the flowing current increased, while the impulse's length was maintained on the same level. Especially when the value of the maximal stress dropped from 1263 to 538 MPa and the elongation decreased from 0,33 to 0,143, for the parameters no. 8 (50 ms/150 ms) and the highest current density, equalling 55,6 A/mm^2 has been obtained. It is also worth mentioning that, in each case, a lower value of flow stress was observed.

TABLE 3

Experimental parameters

No.	t_d	t_p	ρ [A/mm^2]	T [°C]
1	80 µs	400 µs	22,2	51
2	100 µs	1 ms	22,2	56
3	500 µs	2 ms	27,8	130
4	1 ms	10 ms	27,8	120
5	10 ms	100 ms	27,8	131
6	50 ms	500 ms	38,9	134
7	50 ms	300 ms	44,4	177
8	50 ms	150 ms	55,6	283

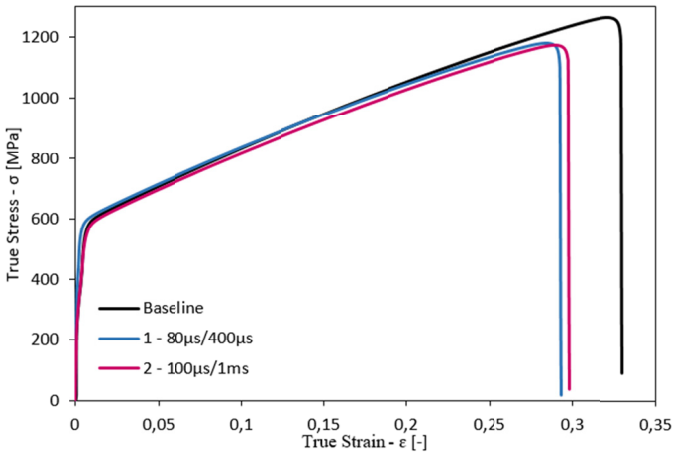

Fig. 3. True stress-strain curves without and with the application of electric current impulses

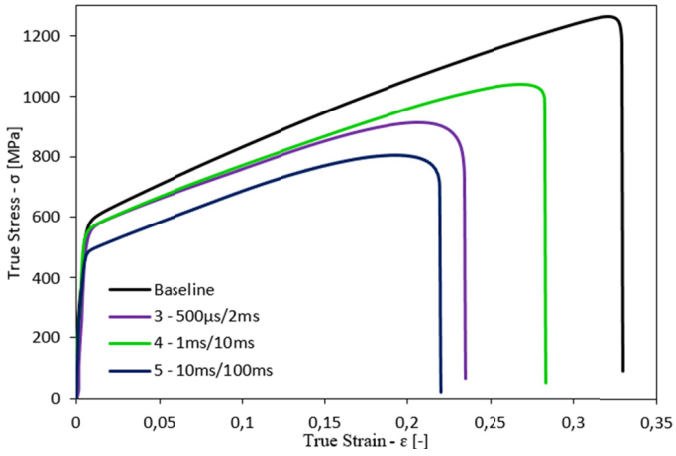

Fig. 4. True stress-strain curves without and with the application of electric current impulses

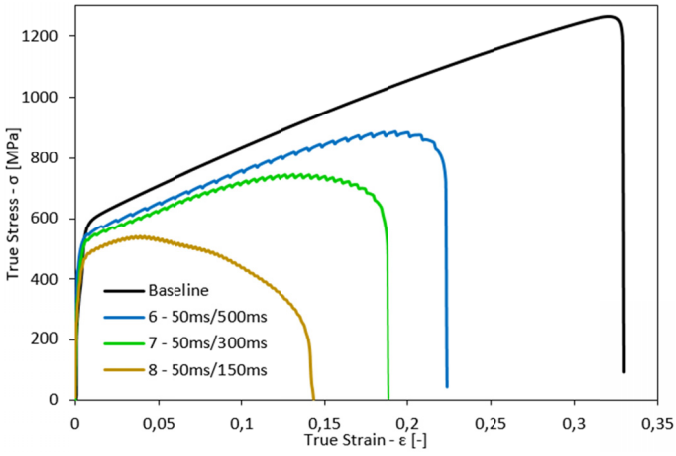

Fig. 5. True stress-strain curves without and with the application of electric current impulses

The curves in Figure 6 and 7 show the differences between the tests made with the application of the electric current and their counterparts made at elevated temperatures. Curves no. 1 and 2 should be compared with the baseline (Fig. 3),

as the temperature of this sample, at the moment of fracture, equalled 45°C, which was caused by the energy of plastic strain, transformed into heat. The baseline curve is characterized by larger elongation and slightly higher flow stress. As it has been shown in Figure 6, a similar situation can be observed in the comparison of the 130°C curve with curves no. 3-6, except line no. 5. The stress value remained at the same level; however, the elongation became significantly reduced. Curve no. 5, in its whole plasticity range, is located below the 130°C curve. The value of yield stress, flow stress and elongation is lower. As shown in Fig. 7, despite the fact that the yield point is at the same level in both curves, no. 8 and 283°C, the elongation of the second is more than twice higher. Nevertheless, the flow stress is significantly lower, except for the initial scope. The temperature equivalent for curve no. 7 was not made; however, its thermal counterpart has intermediate properties in respect of curves no. 5 and 8.

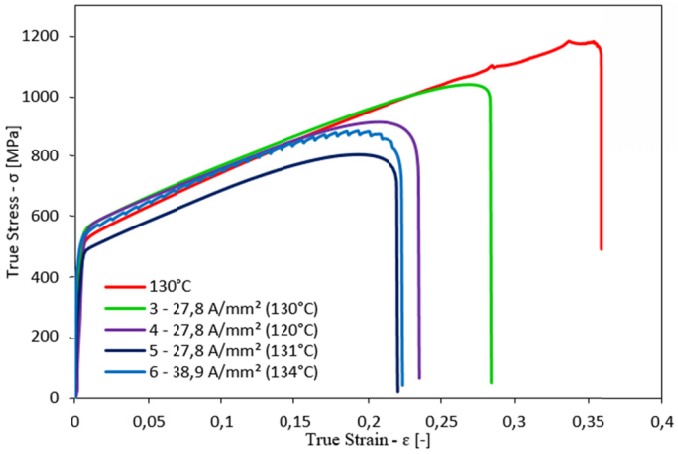

Fig. 6. True stress-strain curves under different conditions

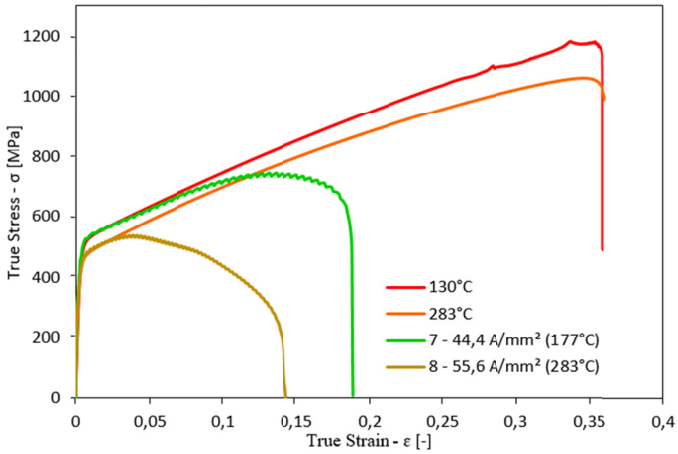

Fig. 7. True stress-strain curves under different conditions

It is worth mentioning that the material stretched at the temperatures of 130 and 283°C was at an elevated temperature during the whole test, while the material with the application of electric current impulses was at room temperature in the initial stage and reached the maximal temperature at the final stage.

Based on the obtained results, it can be stated that, in the examined material, in samples no. 1-4 and 6, the electroplastic effect did not occur, and the drop of stress was caused only by Joule heat. The samples with the application of shorter electric current impulses are characterized by flow stress being on the same level as their thermal counterpart. Smaller elongation of theses samples have an negative characteristics. In the comparison of curves no. 5, 7 and 8 and their temperature equivalents, despite a significant reduction of elongation, a substantial drop of stress was observed, which proves the occurrence of the electroplastic effect in the examined samples. This drop cannot be explained by an increase of temperature.

Figures 8-11 show the morphology of the fractures obtained from scanning microscopy. The microscope worked in the SE (secondary electrons) mode, with the accelerating voltage of 30 kV. Among the samples which reached the largest elongation (e.g. the baseline – Fig. 8 and the 283°C sample – Fig. 11), the presence of the highest and deepest micro-tunnels was observed, which were the effect of a large elongation of the material. As it has been shown in Fig. 10, the micro-tunnels in the samples through which current of higher density was flowed and characterized in a more oval shape, as well as a smaller depth and diameter. Additionally, on the surface of the fractures of these samples, a much higher number of micro-tunnels was observed, whose presence can be connected with the fact that these samples characterized in a larger narrowing of the neck, despite the smaller elongation. The size and depth of the voids on the surface of the fractures were also larger in the case of the samples with a larger elongation. The samples through which current of lower density was flowing characterized in intermediate properties (Fig. 9). The large number of micro-tunnels as well as the much more rapid and larger narrowing of the neck could have been the cause of a smaller elongation and, as a result, a more

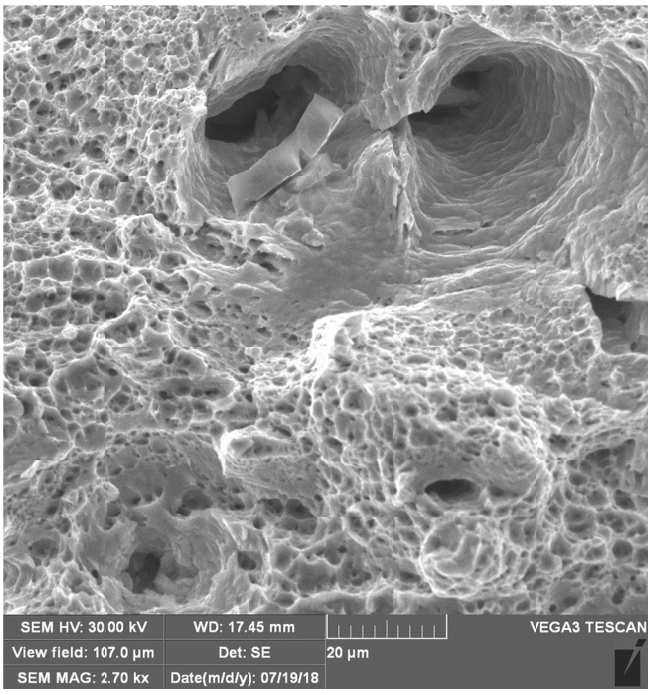

Fig. 8. Morphology of the baseline sample fracture

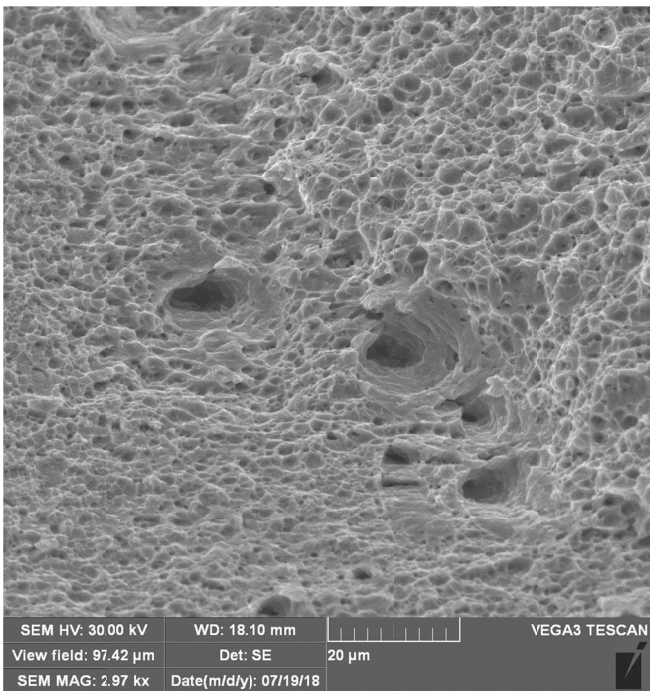

Fig. 9. Morphology of the fracture of sample no. 1

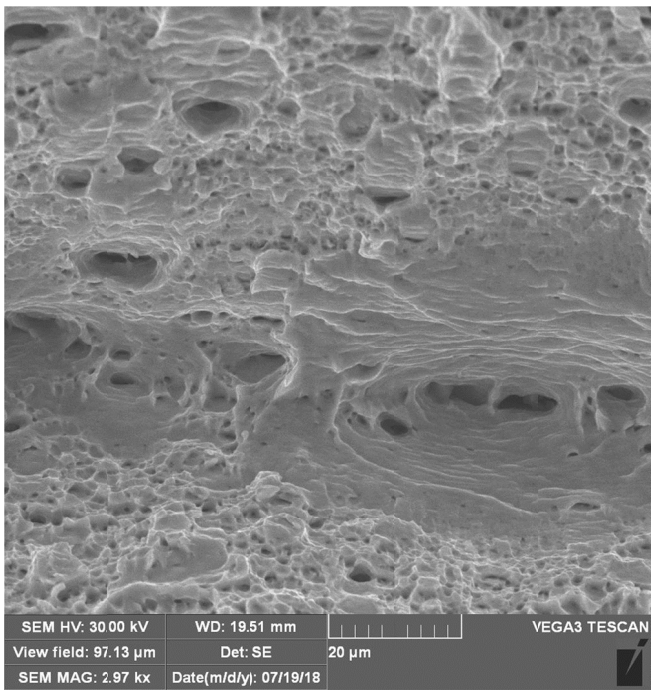

Fig. 11. Morphology of the fracture of sample 280°C

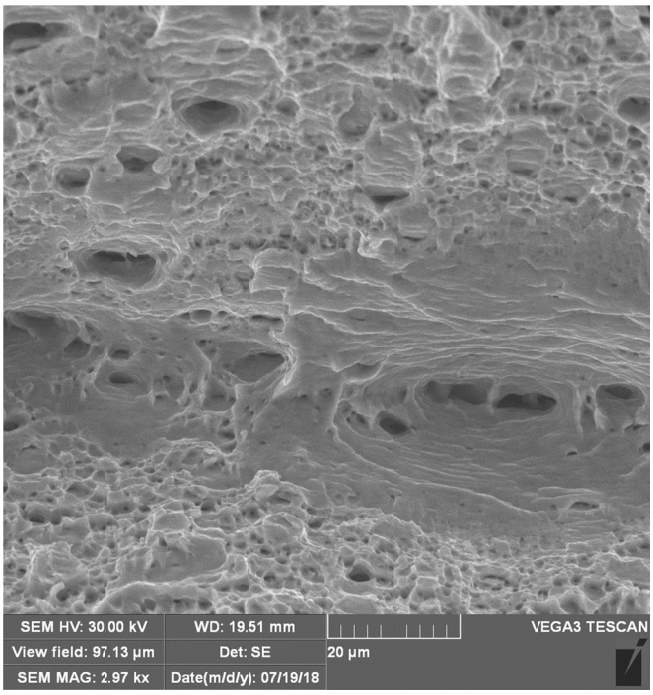

Fig. 10. Morphology of the fracture of sample no. 7

Fig. 12. Microstructure of the baseline sample, LOM, etched in nital

Fig. 13. Microstructure of sample 280°C, LOM, etched in nital

rapid fracture of the material, through which current of higher density was flowing.

The observation was carried out in order to evaluate the microstructural evolution of deformed zones at different conditions (Fig. 12-14). In case of each micrograph the direction of tensile force is parallel to horizontal direction of the picture and banding of the microstructure. Due a strong deformation and banding of the microstructure it is very difficult to identify its evolution. However, figure 13 shows deformation zone of

sample investigated at elevated temperature, it is seen that examples small groups of slip bands are inclined at the angle of 45° to the direction of tensile force (marked by black arrows). That slip systems (in the grains interior) were activated by plastic deformation. Mechanical twins, which occur at such a high level of deformation in this type of steel are not visible. Also the strain-induced martenstie and differences in the grains size were not observed. TEM observation should be carry out to further studying the microstructural evolution, especially to revealing the mechanical twins and their intensity depending on the conditions and eventual confirming the absence of martensite. Moreover, in the each of micrographs presence of the voids, in the form of black dots, were observed. They are identified with micro-tunnels, which were found in the images of fractures (Fig. 8-11). Additionally, in the case of samples deformed with application of current impulses, near the edge of the fractures, the specific bands were revealed, inclined at the angle of 135° to the direction of tensile force (marked by black arrows in Fig. 14).

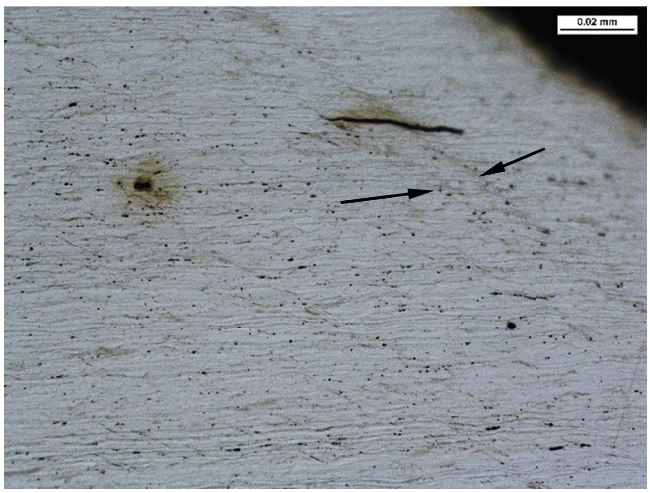

Fig. 14. Microstructure of sample no. 6, LOM, etched in nital

Similar results to those obtained in this study have been achieved by other authors, who examined steels from the AHSS group. A reduction of elongation was observed both in the case of dual-phase and multi-phase steel. Additionally, the application of one long impulse made it possible to reduce the flow stress [14-16]. A continuation of the research on the use of electric current impulses in high-manganese austenitic steels is necessary. Despite the lack of an effective mathematical model describing the electroplastic effect and the side effects of the electric current (Joule heat, reduction of elongation), this solution can be a promising technology in the future, used of the process of pressing sheets made of this type of alloys. It is also worth noting that the obtained current density could have been insufficient for a certain threshold value, recommended for steel. The value is approximately 4 times smaller than the one obtained [1,2]. This can be the reason for the material's reduced plasticity.

4. Conclusion

The study has discussed the results of the investigations performed on high manganese austenitic steel subjected to the test of uniaxial tension with a simultaneous application of electric current impulses. As a result of this, the electroplastic effect occurred in the examined material, which caused its drop of flow stress and elongation. This effect was observed in the case when the current density was higher than 30 A/mm^2, particularly for sample no. 8, for which flow stress reduction was significant. When the current density was lower, EPE did not occur and flow stress reduction was only caused by thermal effect. In order to prove the real influence of the electroplastic effect, the samples were stretched also at the elevated temperatures, analogical to those obtained with the impulse current flow. The performed tests of the samples' fractures showed significant differences in the morphologies of their surfaces, especially in case of the magnitude of neck and size, number and depth of micro-tunnels and voids. However, their differences were not observed in the images of microstructures. Electroplastic deformation of high manganese austenitic steel could be very promising technology. Application of electric current impulses, allow to obtain the same plastic strain with smaller values of forces and hence reduction of the energy consumption. Although it leads to significant decrease of maximum plastic strain, what is very important issue in industrial applications, its strain still remain on quite good level.

REFERENCES

[1] H. Conrad, Mater. Res. Innovat. **2** (1), 1-8 (1998).
[2] H. Conrad, Mater. Sci. Eng. A **322** (1-2), 100-107 (2002).
[3] M. Molotskii, Mater. Sci. Eng. A **322** (2), 248-258 (2000).
[4] J. Song, I. Jang, S. Gwak, J. Bang, Y. Kim, J. Lim, C. Lim, J. Seo, Key Eng. Mater. **744**, 254-258 (2017).
[5] G. Lesiuk, Z. Zimniak, W. Wiśniewski, J.A.F.O. Correia, Procedia Engineer **5**, 928-934 (2016).
[6] Z. Zimniak, G. Radkiewicz, Arch. Civ. Mech. Eng. **8** (2), 173-179 (2008).
[7] K.F. Yao, J. Wang, M. Zheng, P. Yu, H. Zang, Scrpta. Mater. **45** (5), 533-539 (2001).
[8] G. Tang, J. Zhang, Y. Yan, H. Zhou, W. Fang, J. Mater. Process. Tech. **137** (1-3), 96-99 (2003).
[9] M. Breda, F. Michieletto, E. Beridze, C. Gennari, Appl. Mech. Mater. **792**, 568-571 (2015).
[10] D. Kuc, E. Hadasik, G. Niewielski, I. Schindler, E. Mazancová, S. Rusz, P. Kawulok, Arch. Civ. Mech. Eng. **12** (3), 312-317 (2012).
[11] S. Lasek, E. Mazancová, Metalurgija **52** (4), 441-444 (2011).
[12] M. Jabłońska, A. Śmiglewicz, Metalurgija **54** (4), 619-622 (2015).
[13] J.H. Song, J. Lee, I. Hwang, Y.B. Kim, S. Choi, G.A. Lee, M.J. Kang, Appl. Mech. Mater. **389**, 284-288 (2013).
[14] N.T. Thien, Y.-H. Jeong, S-T. Hong, M.-J. Kim, H.N. Han, M.-G. Lee, Inter. J. Precis. Eng. Man. **3** (4), 325-333 (2016).
[15] M.S. Kim, N.T. Vinh, H.-H. Yu, S.-T. Hong, H.-W. Lee, M.-J. Kim, H.N. Han, J.T. Roth, Inter. J. Precis. Eng. Man. **15** (6), 1207-1213 (2016).
[16] J. Magargee, R. Fan, J. Cao, J. Man. Sci. Eng. **135** (6), (2013).